Available online at www.sciencedirect.com
SCIENCE DIRECT®
International Journal of Heat and Mass Transfer 47 (2004) 1937–1951
International Journal of HEAT and MASS TRANSFER
www.elsevier.com/locate/ijhmt

Perturbation analysis to the nonlinear stability characterization of thin condensate falling film on the outer surface of a rotating vertical cylinder

C.I. Chen [a,*], C.K. Chen [b], Y.T. Yang [b]

[a] Department of Industrial Engineering and Management, I-Shou University, 1, Section 1, Hsueh-Cheng Rd., Ta-Hsu Hsiang, Kaohsiung County 84041, Taiwan, ROC

[b] Department of Mechanical Engineering, National Cheng Kung University, Tainan 70101, Taiwan, ROC

Received 22 November 2002; received in revised form 16 September 2003

Abstract

The linear and nonlinear stability theories for characterization of condensate film flow down on the outer surface of a rotating infinite vertical cylinder is investigated analytically. A generalized nonlinear kinematic model is derived to represent the physical system and is solved by the long-wave perturbation method in a two-step procedure. In the first step, the normal mode method is used to characterize the linear behaviors. The amplitude growth rates and the threshold conditions are characterized subsequently and summarized as the by-products of the linear solutions. In the second step, an elaborated nonlinear film flow model is solved by using the method of multiple scales to characterize flow behaviors at various states of sub-critical stability, sub-critical instability, supercritical stability and supercritical explosion. The modeling results indicate that by increasing the rotation speed, Ω, and decreasing the radius of cylinder, R, the film flow becomes less stable, generally.

Keywords: Condensate; Rotation number; Centrifugal force; Ginzburg–Landau equation

1. Introduction

Laminar film condensate on a moving substrate has many engineering application, such as heat exchangers, condensers, nuclear reactors. For example, the rotational cylinder condenser is widely used in paper mills as a paper drum. Steam is fed into a rotating cylinder, on the outer surface of which moist paper is bound and is caused to move with the cylinder surface. Because the temperature of the moist paper is lower than the saturation temperature of steam, the vapor condensates. As a result, a condensate film is formed. The condensate film flow easily forms waves, ripples or some other time-dependent phenomena. The waves, propagating at the film surface, increase the interfacial transfers.

The theory of laminar condensate film flow induced by gravity was firstly developed by Nusselt [1], but the stability problem of condensate falling flow had never been investigated until 1970s. Bankoff [2] used the long-wave perturbation method to study the linear instability problem of the condensate film flow. Without considering the temperature disturbance, the result showed that film condensation on a vertical wall is always unstable. Marschall et al. [3] accounted the disturbances in the temperature field and predicted the existence of a critical Reynolds number below which the condensate film flow is stable. They concluded the condensation will stabilize the film flow, while evaporation destabilize the flow. In previous studies, the mass transfer due to phase

* Corresponding author. Tel.: +886-7-6577711x5522; fax: +886-7-6578536.
E-mail address: eddychen@isu.edu.tw (C.I. Chen).

0017-9310/$ - see front matter © 2003 Elsevier Ltd. All rights reserved.
doi:10.1016/j.ijheatmasstransfer.2003.09.032

Nomenclature

C_p	specific heat of fluid
d	complex wave celerity $= d_r + \mathrm{i}d_i$
g	gravitational acceleration
h^*	film thickness
h_0^*	local base flow film thickness
h_{fg}	latent heat
K	thermal conductivity of the fluid
Nd	dimensionless parameter $= (1-\beta)\xi^2/\beta Pr^2$
p^*	fluid pressure
p_{g}^*	vapor pressure
Pe	local Peclect number $= PrRe$
Pr	Prandtl number $= \rho v C_p/K$
R^*	radius of cylinder
Re	Reynolds number $= u_0^* h_0^*/v$
Ro	Rotation number $= \Omega^* h_0^*/u_0^*$
r^*, z^*	coordinates transverse to and along the cylinder surface
S^*	surface tension of the fluid
t^*	time
T^*	fluid temperature
T_{s}^*	vapor saturation temperature
T_{w}^*	wall temperature
u_0^*	reference velocity $= gh_0^{*2}/4v\Gamma$
u^*, v^*, w^*	velocities along r^*-, θ^*- and z^*-directions, respectively

Greek symbols

α	dimensionless wave number
β	density ratio $= \rho_{\mathrm{g}}/\rho$
ε	infinitesimal parameter
ξ	Jakob number $= C_p(T_{\mathrm{s}}^* - T_{\mathrm{w}}^*)/h_{\mathrm{fg}}$
η	dimensionless perturbed film thickness
θ	dimensionless temperature
λ	perturbed wave length
μ	fluid dynamic viscosity
v	fluid kinematic viscosity
ρ	fluid density
ρ_{g}	vapor density
Ω^*	constant angular velocity.
φ	stream function

Superscripts

*	dimensional quantities
$'$	differentiation with respect to h

Subscripts

t, r, z	partial differentiation with respect to the subscript
$0, 1, 2, \ldots$	expansion order of the long wave

change at the interface was not considered. Ünsal [4] modified the kinematic condition by using the interfacial energy balance equation, and found the finite critical Reynolds number for the vertical wall. Essentially, the linear stability analysis can only be applied to study the cases of infinitesimal disturbances. When disturbance grows to be of a finite value, linear stability theory becomes invalid.

Benney [5] studied the nonlinear evolution equation for free surfaces of the film flows by using the method of small parameters. The solutions thus obtained can be used to predict nonlinear instability conditions. However, the solutions cannot be used to predict supercritical stability since the influence of surface tension is neglected in the modeling process. The effect of surface tension was studied by Lin [6], Nakaya [7] and Krishna et al. [8] who considered it as one of the necessary condition and treated it in terms of zeroth order terms. Hwang and Weng [9] showed that the conditions of both supercritical stability and sub-critical instability are possible to occur for a film flow system.

Extensive studies on the hydrodynamic stability problems regarding the fluid films flowing down a vertical cylinder surface have already investigated by several researchers. Krantz et al. [10] presented an asymptotic solution and pointed out that the effect of curvature on the stability of the film flow is indeed significant. Rosenau and Oron [11] derived an amplitude equation which describes the evolution of a disturbed free film surface traveling down an infinite vertical cylindrical column. The numerical modeling results indicated that both conditions of supercritical stability and sub-critical instability are possible to occur for the film flow. Hung et al. [12] investigated the weakly nonlinear stability analysis of a condensate film flowing down a vertical cylinder. They also showed that supercritical stability in the linearly unstable region and sub-critical instability in the linearly stable region can co-exist. They also indicated that the lateral curvature of the cylinder has the destabilizing effect on the film flow stability.

It was found that the stability problem of practical condensate film flows to the outer surface of a rotating vertical cylinder has not been fully explored so far in literature. These types of stability problems are indeed of great importance to many industrial applications. As the centrifugal force is introduced into the governing equation, the complexity of mathematical calculation is increased. But the results are more compatible with the practical situation.

2. Problem formulation

In this study, the axisymmetric flow of an incompressible, condensate flow on the outer surface of a vertical cylinder which rotates with a constant velocity Ω^* is considered. The asterisk represents that this physical parameter is dimensional quantity. The appropriate physical configuration is shown schematically in Fig. 1. In this case, all associated physical properties and the rate of film flow are assumed to be constant (i.e. time-invariant). Cylindrical polar coordinate (r^*, θ^*, z^*) are used, where r^* denotes the radial direction perpendicular to the centerline of the cylinder, θ^* denotes the circumferential direction and z^* denotes the axial direction. The liquid–air interface is located at $r^* = R^* + h^*(z^*, t^*)$, where R^* is the cylinder radius and h^* is the film thickness. Let u^* and w^* be the velocity components in $r^*$and z^* directions, respectively. The equations of continuity, motion and energy can be expressed as

$$\frac{1}{r^*}\frac{\partial(r^*u^*)}{\partial r^*} + \frac{\partial w^*}{\partial z^*} = 0, \tag{1}$$

$$\frac{\partial u^*}{\partial t^*} + u^*\frac{\partial u^*}{\partial r^*} + w^*\frac{\partial u^*}{\partial z^*} - \frac{v^{*2}}{r^*} = -\frac{1}{\rho}\frac{\partial p^*}{\partial r^*} + \frac{\mu}{\rho}\left(\frac{1}{r^*}\frac{\partial}{\partial r^*}\left(r^*\frac{\partial u^*}{\partial r^*}\right) - \frac{u^*}{r^{*2}} + \frac{\partial^2 u^*}{\partial z^{*2}}\right), \tag{2}$$

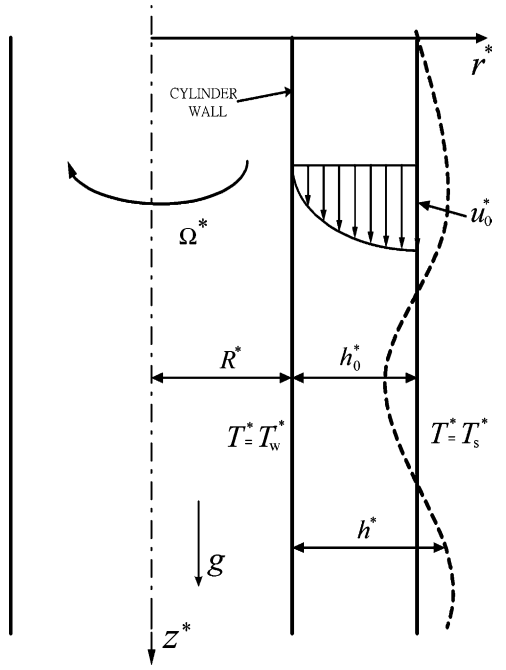

Fig. 1. Schematic diagram of a condensate thin film flow traveling down along a rotating vertical cylinder.

$$\frac{\partial w^*}{\partial t^*} + u^*\frac{\partial w^*}{\partial r^*} + w^*\frac{\partial w^*}{\partial z^*} = -\frac{1}{\rho}\frac{\partial p^*}{\partial z^*} + g + \frac{\mu}{\rho}\left(\frac{1}{r^*}\frac{\partial}{\partial r^*}\left(r^*\frac{\partial w^*}{\partial r^*}\right) + \frac{\partial^2 w^*}{\partial z^{*2}}\right), \tag{3}$$

$$\frac{\partial T^*}{\partial t^*} + u^*\frac{\partial T^*}{\partial r^*} + w^*\frac{\partial T^*}{\partial z^*} = \frac{K}{\rho C_p}\left(\frac{1}{r^*}\frac{\partial}{\partial r^*}\left(r^*\frac{\partial T^*}{\partial r^*}\right) + \frac{\partial^2 T^*}{\partial z^{*2}}\right), \tag{4}$$

where T^*, ρ, p^*, μ, C_p and K are the fluid temperature, density, pressure, dynamic viscosity, specific heat and the thermal conductivity of the fluid, respectively.

The thickness of film flowing down on the cylinder inner wall is measured by Takamasa and Kobayashi [13] and the result shows the film is very thin. In consequence it is reasonable to assume that the tangential velocity is constant throughout the radial direction in the thin film, i.e. $v^* = R^*\Omega^*$.

The boundary conditions on the wall of the cylinder at $r^* = R^*$ are given as

$$u^* = 0, \quad w^* = 0, \quad T^* = T_w^*. \tag{5}$$

The boundary conditions at free surface of $r^* = R^* + h^*$ are derived based on the results given by Edwards et al. [14]. The vanishing of shear and normal stresses on free surface give another boundary condition and the free surface temperature is assumed to the same as the vapor saturation temperature.

$$2\left(\frac{\partial u^*}{\partial r^*} - \frac{\partial w^*}{\partial z^*}\right)\frac{\partial h^*}{\partial z^*} + \left(\frac{\partial u^*}{\partial z^*} + \frac{\partial w^*}{\partial r^*}\right)\left[1 - \left(\frac{\partial h^*}{\partial z^*}\right)^2\right] = 0, \tag{6}$$

$$P^* + \frac{k^2(\beta-1)}{h_{fg}^2\rho\beta}\left(\frac{\partial T^*}{\partial r^*} - \frac{\partial h^*}{\partial z^*}\frac{\partial T^*}{\partial z^*}\right)^2\left[1 + \left(\frac{\partial h^*}{\partial z^*}\right)^2\right]^{-1} - 2\rho\nu\left[\frac{\partial u^*}{\partial r^*} - \left(\frac{\partial w^*}{\partial r^*} + \frac{\partial u^*}{\partial z^*}\right)\frac{\partial h^*}{\partial z^*} + \frac{\partial w^*}{\partial z^*}\left(\frac{\partial h^*}{\partial z^*}\right)^2\right] \times \left[1 + \left(\frac{\partial h^*}{\partial z^*}\right)^2\right]^{-1} + S^*\left\{\frac{\partial^2 h^*}{\partial z^{*2}}\left[1 + \left(\frac{\partial h^*}{\partial z^*}\right)^2\right]^{-3/2} - \frac{1}{r}\left[1 + \left(\frac{\partial h^*}{\partial z^*}\right)^2\right]^{-1/2}\right\} = p_g^*, \tag{7}$$

$$T^* = T_s^*. \tag{8}$$

The kinematic condition that the flow cannot travel across a free surface can be described as

$$K\left(\frac{\partial T^*}{\partial r^*} - \frac{\partial T^*}{\partial z^*}\frac{\partial h^*}{\partial z^*}\right) + \rho h_{fg}\left(u^* - w\frac{\partial h^*}{\partial z^*} - \frac{\partial h^*}{\partial t^*}\right) = 0, \tag{9}$$

where T_s^* is vapor saturation temperature, T_w^* is wall temperature, p_g^* is the vapor pressure, S^* is the surface tension and h_{fg} is the latent heat of phase change. By introducing the stream function, φ^*, into dimensional velocity components, they become

$$u^* = \frac{1}{r^*}\frac{\partial \varphi^*}{\partial z^*}, \quad w^* = -\frac{1}{r^*}\frac{\partial \varphi^*}{\partial r^*}. \tag{10}$$

It is customarily to define flow associated dimensionless quantities as

$$z = \frac{\alpha z^*}{h_0^*}, \quad r = \frac{r^*}{h_0^*}, \quad R = \frac{R^*}{h_0^*}, \quad t = \frac{\alpha u_0^* t^*}{h_0^*}, \quad h = \frac{h^*}{h_0^*},$$
$$\varphi = \frac{\varphi^*}{u_0^* h_0^{*2}}, \quad p = \frac{p^* - p_g^*}{\rho u_0^{*2}}, \quad Re = \frac{u_0^* h_0^*}{\nu},$$
$$S = \left(\frac{S^{*3}}{2^4 \rho^3 \nu^4 g}\right)^{1/3}, \quad \alpha = \frac{2\pi h_0^*}{\lambda}, \quad \theta = \frac{T^* - T_w^*}{T_s^* - T_w^*},$$
$$Pr = \frac{\rho \nu C_p}{K}, \quad Pe = PrRe, \quad Nd = \frac{(1-\beta)\xi^2}{\beta Pr^2}, \tag{11}$$

where h_0^* is the constant film thickness of local base flow, g is the gravitational acceleration, Pr is the Prandtl number, Pe is the Peclect number, Re is the Reynolds number, R is the dimensionless radius of the cylinder, φ is dimensionless stream function, S is dimensionless surface tension, α is the dimensionless wave number, ξ is the Jakob number, β is density ratio, θ is dimensionless temperature and λ is the wavelength. u_0^* is the reference velocity and can be expressed as [15]

$$u_0^* = \frac{g h_0^{*2}}{4\nu\Gamma}, \tag{12}$$

where $\Gamma = \left[2(1+R)^2 \ln\left(\frac{1+R}{R}\right) - (1+2R)\right]^{-1}$.

In order to investigate the effect of angular velocity, Ω^*, on the stability of the flow field, the dimensionless parameter, Rotation number, is introduced

$$Ro = \frac{\Omega^* h_0^*}{u_0^*}. \tag{13}$$

Assuming that $\alpha \ll 1$, the nondimensional governing equations and the associated boundary conditions can be expressed as

$$p_r = \alpha[Re^{-1}(r^{-1}\varphi_{rrz} - r^{-2}\varphi_{rz})] + Ro^2\frac{R^2}{r} + O(\alpha^2), \tag{14}$$

$$r^{-1}(r(r^{-1}\varphi_r)_r)_r = 4\Gamma + \alpha Re(-p_z + r^{-1}\varphi_{tr} + r^{-2}\varphi_z\varphi_{rr} - r^{-3}\varphi_z\varphi_r - r^{-2}\varphi_r\varphi_{rz}) + O(\alpha^2), \tag{15}$$

$$r^{-1}(r\theta_r)_r = \alpha Pe(\theta_t - r^{-1}\varphi_r\theta_z + r^{-1}\varphi_z\theta_r) + O(\alpha^2). \tag{16}$$

At the cylinder surface ($r = R$)

$$\varphi_r = \varphi_z = \theta = 0, \tag{17}$$

and at free surface ($r = R + h$)

$$(r^{-1}\varphi_r)_r = O(\alpha^2), \tag{18}$$

$$p = -2S \cdot Re^{-5/3}(2\Gamma)^{1/3}(\alpha^2 h_{zz} - r^{-1}) + \alpha\{-2Re^{-1}[(r^{-2}\varphi_r - r^{-1}\varphi_{rr})h_z + r^{-2}\varphi_z - r^{-1}\varphi_{rz}]\} - Nd \cdot Re^{-2} \cdot \theta_r^2 + O(\alpha^2), \tag{19}$$

$$\theta = 1, \tag{20}$$

$$\xi \cdot (\theta_r - \alpha^2\theta_z h_z) + \alpha Pe(r^{-1}\varphi_z + r^{-1}\varphi_r h_z - h_t) = 0. \tag{21}$$

The subscripts r, z, rr, zz and rz are used to represent various partial derivatives of the associated underlying variables.

Since the modes of long-wavelength that gives the smallest wave number are most likely to induce flow instability for the film flow [16,17], the dimensionless wave number of the long-wavelength mode, α, can then be chosen as the perturbation parameter for variable expansion. By so doing the stream function, flow pressure and temperature can be perturbed and represented as

$$\varphi = \varphi_0 + \alpha\varphi_1 + O(\alpha^2), \quad p = p_0 + \alpha p_1 + O(\alpha^2),$$
$$\theta = \theta_0 + \alpha\theta_1 + O(\alpha^2). \tag{22}$$

The flow conditions of the thin film can be obtained by inserting above expressions into Eqs. (14)–(21) and then solving systematically the resulting equations. In practice, the nondimensional surface tension S is a large value; the term $\alpha^2 S$ can be treated as a quantity of zeroth order [12,18]. By careful calculation, the zeroth order and first order solutions can be obtained and are given in Appendix A. The zeroth and the first order solutions are then inserted into the dimensionless free surface kinematic equation to yield the following generalized nonlinear kinematic equation

$$h_t + X(h) + A(h)h_z + B(h)h_{zz} + C(h)h_{zzzz} + D(h)h_z^2 + E(h)h_z h_{zzz} = 0, \tag{23}$$

where $X(h)$, $A(h)$, $B(h)$, $D(h)$ and $E(h)$ are given in Appendix B.

3. Stability analysis

The dimensionless film thickness when expressed in perturbed state can be given as

$$h(t,z) = 1 + \eta(t,z), \tag{24}$$

where η is a perturbed quantity to the stationary film thickness. By inserting Eq. (24) into Eq. (23) and collecting all terms up to the order of η^3, the evolution equation of η becomes

$$\eta_t + X'\eta + A\eta_z + B\eta_{zz} + C\eta_{zzzz} + D\eta_z^2 + E\eta_z\eta_{zzz} = -\left[\frac{X''}{2}\eta^2 + \frac{X'''}{6}\eta^3 + \left(A'\eta + \frac{A''}{2}\eta^2\right)\eta_z + \left(B'\eta + \frac{B''}{2}\eta^2\right)\eta_{zz} + \left(C'\eta + \frac{C''}{2}\eta^2\right)\eta_{zzzz} + (D + D'\eta)\eta_z^2 + (E + E'\eta)\eta_z\eta_{zzz}\right] + \mathrm{O}(\eta^4). \quad (25)$$

The values of X, A, B, C, D and E and their derivatives are all evaluated at the dimensionless height, $h = 1$, of the film flow.

3.1. Linear stability analysis

As the nonlinear terms in Eq. (25) are neglected, the linearized equation is obtained as

$$\eta_t + X'\eta + A\eta_z + B\eta_{zz} + C\eta_{zzzz} = 0. \quad (26)$$

The normal mode analysis method can be performed by assuming that

$$\eta = a\exp[\mathrm{i}(z - dt)] + \mathrm{c.c.}, \quad (27)$$

where a is the perturbation amplitude and c.c. is the complex conjugate counterpart. The complex wave celerity, d, is given as

$$d = d_r + \mathrm{i}d_i = A + \mathrm{i}(B - C - X'), \quad (28)$$

where d_r is the linear wave speed and d_i is the linear growth rate of the wave amplitudes. The flow is in linearly unstable condition if $d_i > 0$, and is in linearly stable condition if $d_i < 0$.

3.2. Nonlinear stability analysis

In order to characterize the nonlinear behaviors of thin film flows, the method of multiple scales [8] is employed here and presented as

$$\frac{\partial}{\partial t} \to \frac{\partial}{\partial t} + \varepsilon\frac{\partial}{\partial t_1} + \varepsilon^2\frac{\partial}{\partial t_2}, \quad (29)$$

$$\frac{\partial}{\partial z} \to \frac{\partial}{\partial z} + \varepsilon\frac{\partial}{\partial z_1}, \quad (30)$$

$$\eta(\varepsilon, z, z_1, t, t_1, t_2) = \varepsilon\eta_1 + \varepsilon^2\eta_2 + \varepsilon^3\eta_3, \quad (31)$$

where ε is a small perturbation parameter. The perturbed variable as expressed in terms of the perturbation parameter is given as

$$(L_0 + \varepsilon L_1 + \varepsilon^2 L_2)(\varepsilon\eta_1 + \varepsilon^2\eta_2 + \varepsilon^3\eta_3) = -\varepsilon^2 N_2 - \varepsilon^3 N_3, \quad (32)$$

where

$$L_0 = \frac{\partial}{\partial t} + X' + A\frac{\partial}{\partial z} + B\frac{\partial}{\partial z^2} + C\frac{\partial}{\partial z^4}, \quad (33)$$

$$L_1 = \frac{\partial}{\partial t_1} + A\frac{\partial}{\partial z_1} + 2B\frac{\partial}{\partial z}\frac{\partial}{\partial z_1} + 4C\frac{\partial^3}{\partial z^3}\frac{\partial}{\partial z_1}, \quad (34)$$

$$L_2 = \frac{\partial}{\partial t_2} + B\frac{\partial^2}{\partial z_1^2} + 6C\frac{\partial^2}{\partial z^2}\frac{\partial^2}{\partial z_1^2}, \quad (35)$$

$$N_2 = \frac{X''}{2}\eta_1^2 + A'\eta_1\eta_{1z} + B'\eta_1\eta_{1zz} + C'\eta_1\eta_{1zzzz} + D\eta_{1z}^2 + E\eta_{1z}\eta_{1zzz}, \quad (36)$$

$$N_3 = X''\eta_1\eta_2 + A'(\eta_1\eta_{2z} + \eta_{1z}\eta_2 + \eta_1\eta_{1z_1}) + B'(\eta_1\eta_{2zz} + 2\eta_1\eta_{1zz_1} + \eta_{1zz}\eta_2) + C'(\eta_1\eta_{2zzzz} + 4\eta_1\eta_{1zzzz_1} + \eta_{1zzzz}\eta_2) + D(2\eta_{1z}\eta_{2z} + 2\eta_{1z}\eta_{1z_1}) + E(\eta_{1z}\eta_{2zzz} + 3\eta_{1z}\eta_{1zzz_1} + \eta_{1zzz}\eta_{2z} + \eta_{1zzz}\eta_{1z_1}) + \tfrac{1}{2}A''\eta_1^2\eta_{1z} + \tfrac{1}{2}B''\eta_1^2\eta_{1zz} + \tfrac{1}{2}C''\eta_1^2\eta_{1zzzz} + D'\eta_1\eta_{1z}^2 + E'\eta_1\eta_{1z}\eta_{1zzz}. \quad (37)$$

Eq. (32) can now be solved order by order. After collecting the terms of order ε and solving for the resulting equation $L_0\eta_1 = 0$, the solution can be easily obtained as

$$\eta_1 = a(z_1, t_1, t_2)\exp[\mathrm{i}(z - d_r t)] + \mathrm{c.c.} \quad (38)$$

Similarly, the solution of η_2 and the secular condition for the equation of order ε^2 can also be derived and given, respectively, as

$$\eta_2 = ea^2\exp[2\mathrm{i}(z - d_r t)] + \mathrm{c.c.} \quad (39)$$

By plugging both η_1 and η_2 into the equation of order ε^3, the resulting equation becomes

$$\frac{\partial a}{\partial t_2} + D_1\frac{\partial^2 a}{\partial z_1^2} - \varepsilon^{-2}d_i a + (E_1 + \mathrm{i}F_1)a^2\bar{a} = 0, \quad (40)$$

where

$$e = e_r + \mathrm{i}e_i = \frac{\left(\frac{X'}{2} - B' + C' - D + E\right)}{16C - 4B + X} + \mathrm{i}\frac{-A'}{16C - 4B + X}, \quad (41)$$

$$D_1 = B - 6C, \quad (42)$$

$$E_1 = (X'' - 5B' + 17C' + 4D - 10E)e_r - A'e_i + \left(\tfrac{1}{2}X'' - \tfrac{3}{2}B'' + \tfrac{3}{2}C'' + D' - E'\right), \quad (43)$$

$$F_1 = (X'' - 5B' + 17C' + 4D - 10E)e_i + A'e_r + \tfrac{1}{2}A''. \quad (44)$$

The overhead bar appeared in the above expressions stands for the complex conjugate of the same variable. Eq. (40) is the so-called Ginzburg–Landau equation [19] and can be used to characterize the nonlinear behaviors of the traveling film flow.

In order for a supercritical stable region to exist in the linearly unstable region ($d_i > 0$), the condition is given as $E_1 > 0$. The associated wave amplitude εa_0 in

the supercritical stable region is obtained and presented as

$$\varepsilon a_0 = \sqrt{\frac{d_i}{E_1}}. \tag{45}$$

The nonlinear wave speed is then derived and given as

$$Nc_r = d_r + d_i\left(\frac{F_1}{E_1}\right). \tag{46}$$

On the other hand, the condition for the film flow to present the behavior of sub-critical instability in the linearly stable region ($d_i < 0$) is given as $E_1 < 0$, and the threshold amplitude of the wave is given as εa_0. The sub-critical stable region can only be found as $E_1 > 0$. The neutral stability curve can only be derived and plotted for the condition of $E_1 = 0$. Based on the above discussion, it is obvious that the Ginzburg–Landau equation can be used to characterize various flow states. The results are summarized and presented in Table 1.

4. Results and discussions

Physical parameters that are selected for study include (1) Reynolds numbers ranging from 0 to 15, (2) the dimensionless perturbation wave numbers ranging from 0 to 0.12, (3) Rotation number including 0, 0.1 and 0.2 and (4) the values of dimensionless radius including 10, 20, 50 and 100. By setting $d_i = 0$ in the linear stability analysis, the neutral stability curve can be easily determined from Eq. (28). The α–Re plane is divided into two different characteristic regions by the neutral stability curve. One is the linearly stable region where small disturbances decay with time and the other is the linearly

Table 1
Various states of the Landau equation

Linearly stable (sub-critical region) $d_i < 0$	Sub-critical instability $E_1 < 0$	$\varepsilon a_0 < \left(\frac{d_i}{E_1}\right)^{1/2}$	$a_0 \to 0$	Conditional stability
		$\varepsilon a_0 > \left(\frac{d_i}{E_1}\right)^{1/2}$	$a_0 \uparrow$	Sub-critical explosive state
	Sub-critical (absolute) stability $E_1 > 0$	$a_0 \to 0$		
Linearly unstable (supercritical region) $d_i > 0$	Supercritical explosive state $E_1 < 0$	$a_0 \uparrow$		
	Supercritical stability $E_1 > 0$	$\varepsilon a_0 \to \left(\frac{d_i}{E_1}\right)^{1/2}$ $Nc_r \to d_r + d_i\frac{F_1}{E_1}$		

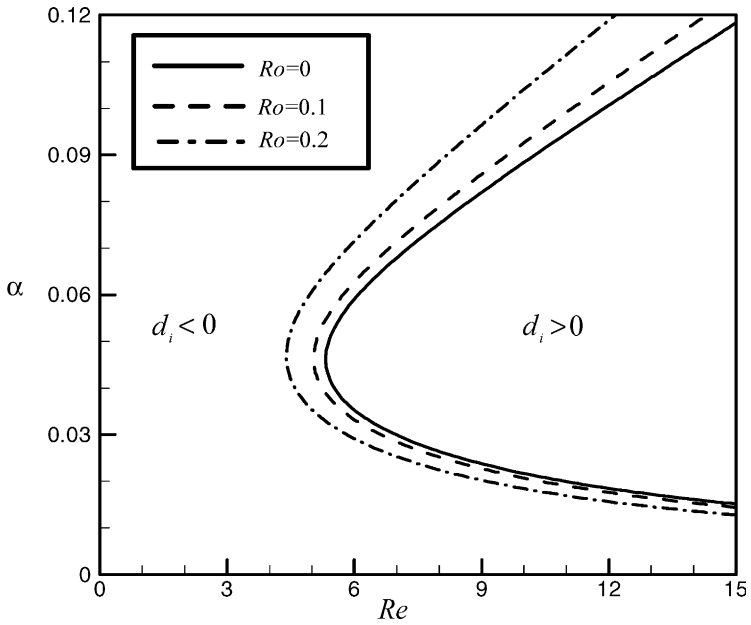

Fig. 2. Neutral stability curves for three different Ro values at $R = 20$.

unstable region where small perturbations grow as time increases. In order to study the influence of rotation and the radius of cylinder on the stability of the film flow, a constant dimensionless surface tension is used throughout for all numerical computations. The value is selected as 6173.5 [15]. The other dimensionless parameters related to fluid properties are selected as Jakob number, $\xi = 0.0872$; Prandtl number, $Pr = 2.62$; and density ratio, $\beta = 0.000611$.

4.1. Linear stability analysis

Fig. 2 shows the neutral stability curves of a condensate falling film flow with various values of Rotation number. The results indicate that the area of linear unstable region ($d_i > 0$) enlarges as the rotating speed increase. Fig. 3(a) shows the effect of radius on the neutral stability curves when $Ro = 0$. The results indicate that the area of linearly unstable region ($d_i > 0$) becomes larger for a decreasing R. Namely, a cylinder with smaller radius induces the flow instability condition. This destabilizing effect occurs because the radius of the trough of wave have a smaller value than that at the crest of waves, and the surface tension will produce large capillary pressure at the smaller radius of curvature. This induces the capillary pressure force tending to move the fluid trough to crest, thus increasing the amplitude of wave. Fig. 3(b) shows the rotation effect ($Ro = 0.1$) on the neutral stability curves. The conclusion of Fig. 3(c) does not hold anymore. As we can tell from the figure, the ability to stabilize the flow field is no longer proportional to the cylinder radius. This is because the rotating motion induces the centrifugal force. This force is defined as the angular velocity multiplied

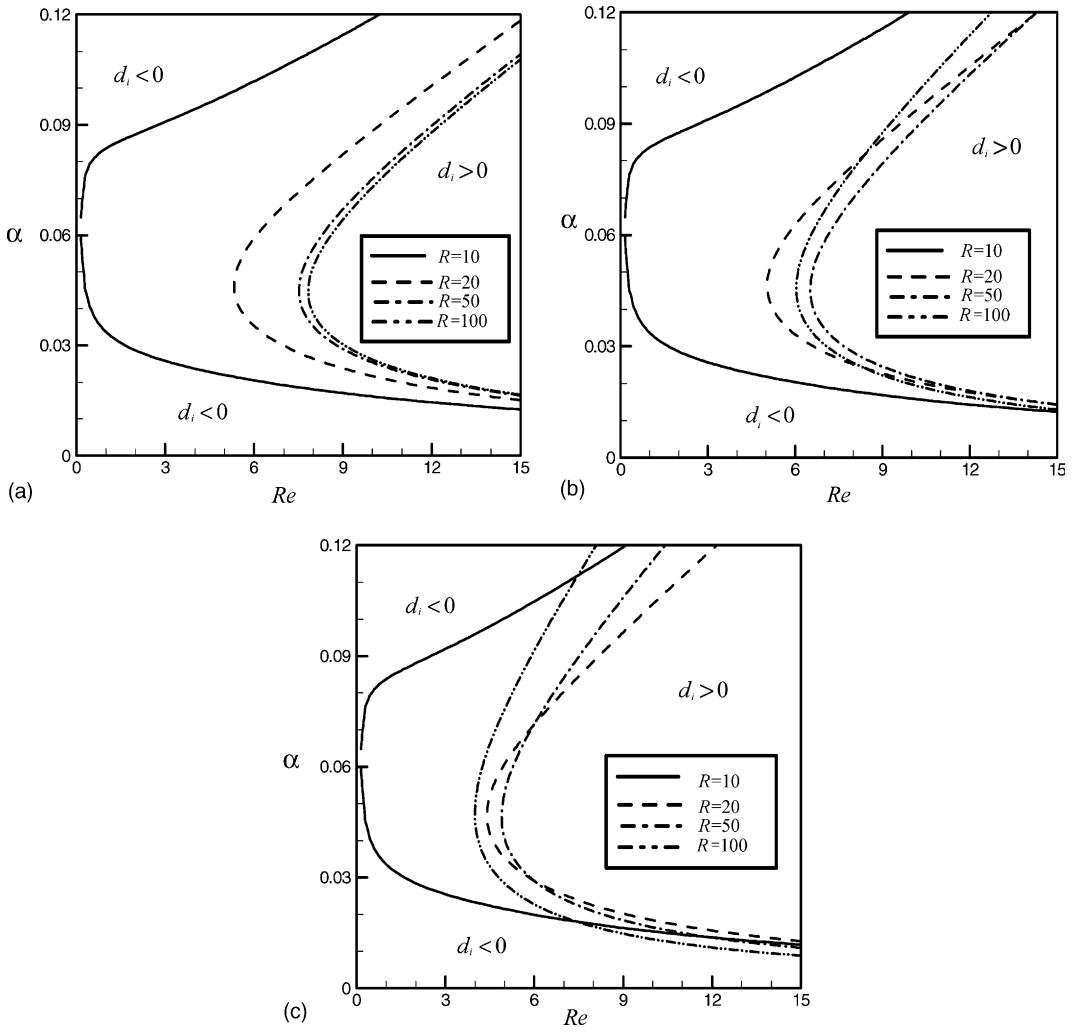

Fig. 3. Neutral stability curves for four different R values at (a) $Ro = 0$; (b) $Ro = 0.1$; (c) $Ro = 0.2$.

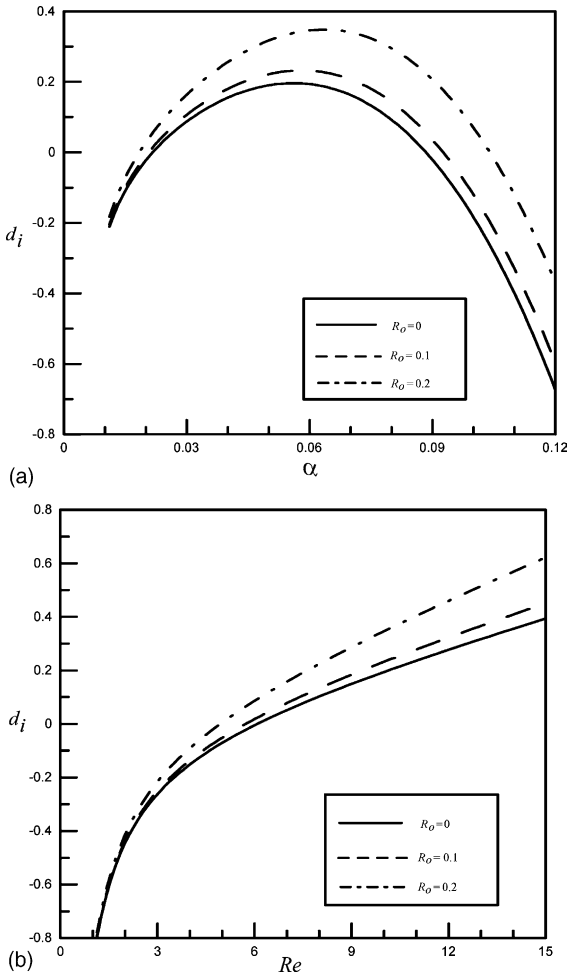

Fig. 4. Amplitude growth rate of disturbed waves in condensate flows for three different Ro values at (a) $Re = 10$, $R = 20$; (b) $\alpha = 0.06$, $R = 20$.

by the cylinder radius and its direction is along with outward of the r-direction. Therefore, it serves as the destabilizing effect on the flow field. On the contrary, the radius itself serves as the stabilizing factor. Once the cylinder starts to rotate, the mutual influence between radius and centrifugal force should be considered. The cylinder with large radius will destabilize further under the rotation motion. In the case of $Ro = 0.2$, Fig. 3(c), the tread of instability for the cylinder with larger radius is much higher than those with smaller ones. Comparing with Figs. 2 and 3(a)–(c), the cylinder with large radius is more stable than the cylinder with smaller one when $Ro = 0$. As the cylinder starts to rotate, the cylinder with large radius is no longer the most stable one. This is because the centrifugal force destabilizes the flow field.

The temporal growth rate of the film flow is also computed by using Eq. (28). Fig. 4(a)–(b) show the temporal film growth rate of a condensate fluid flowing down a rotating cylinder at $Ro = 0.1$, 0.2 and a stationary vertical cylinder (i.e. $Ro = 0$). It is interesting to note that temporal film growth rate decreases as the values of both Ro and Re decrease. Furthermore, it is found that both the wave number of neutral mode and the maximum temporal film growth rate increase as the value of Ro increases. In other words, the larger the value of rotating parameter Ro is, the lower the stability of a liquid film becomes. Fig. 5(a) and (b) show the temporal film growth rate in rotating case of which Rotation number is equal to 0 and 0.1 at various cylinder radius. The result of these two figures is exactly the same as the results of Fig. 3(a) and (b).

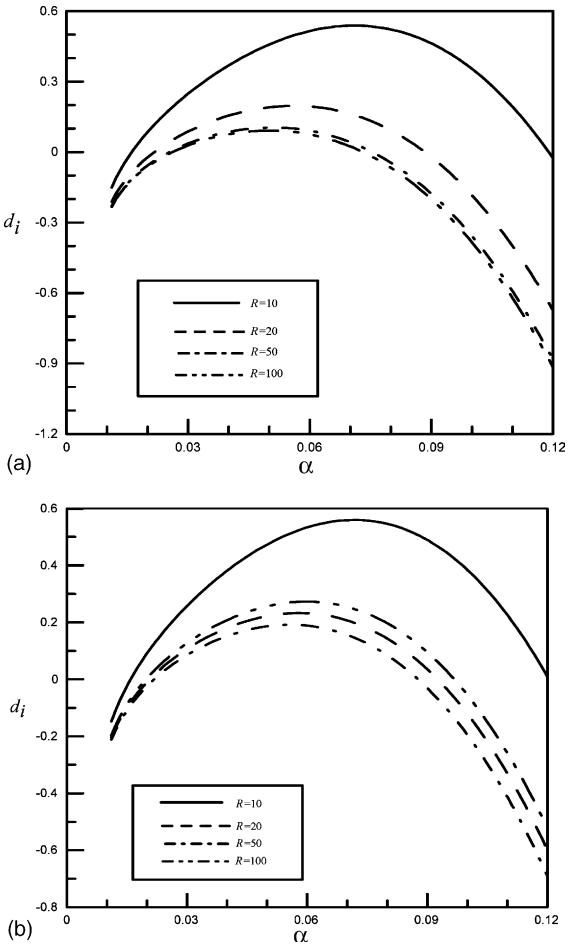

Fig. 5. Amplitude growth rate of disturbed waves in condensate flows for four different R values at (a) $Re = 10$, $Ro = 0$; (b) $Re = 10$, $Ro = 0.1$.

4.2. Nonlinear stability analysis

As the perturbed wave grows to finite amplitude, the linear stability theory is no longer valid for accurate prediction of flow behavior. The nonlinear stability analysis is used here to study the effect of finite-amplitude disturbances on the change of stability behaviors in the linearly stable region. In other words, we are looking for the behavior of sub-critical instability in the linearly stable region by using the nonlinear, instead of linear, flow stability theory. By using the same nonlinear flow stability theory, one can also characterize the flow behaviors that subsequent nonlinear evolution of disturbances in the linearly unstable region may be redeveloped to a new equilibrium state of finite amplitudes (i.e. supercritical stability) or become unstable. The flow instability in the linearly stable region, named sub-critical instability, can be easily realized by setting the variable E_1 in Eq. (43) to a negative value. In other words, if $E_1 < 0$, the amplitude of disturbed waves in the linearly stable region is possible to develop to a unstable state, even though the prediction obtained by linear analysis always gives stable result. The hatched areas in Fig. 6(a)–(d) reveal that various conditions for the sub-critical instability $(d_i < 0, E_1 < 0)$, the sub-critical stability$(d_i < 0, E_1 > 0)$, the supercritical stability $(d_i > 0, E_1 > 0)$ and the explosive supercritical instability $(d_i > 0, E_1 < 0)$ are possibly to occur for different rotating speed.

Fig. 6(a)–(b) show that the neutral stability curves of $d_i = 0$ and $E_1 = 0$ are shifted as the values of Ro increase. Therefore, the area of shaded sub-critical instability region $(d_i < 0, E_1 < 0)$ decreases and the area of shaded supercritical instability region $(d_i > 0, E_1 < 0)$ increases as the values of Ro increase. The area of supercritical stability region $(d_i > 0, E_1 > 0)$ increases

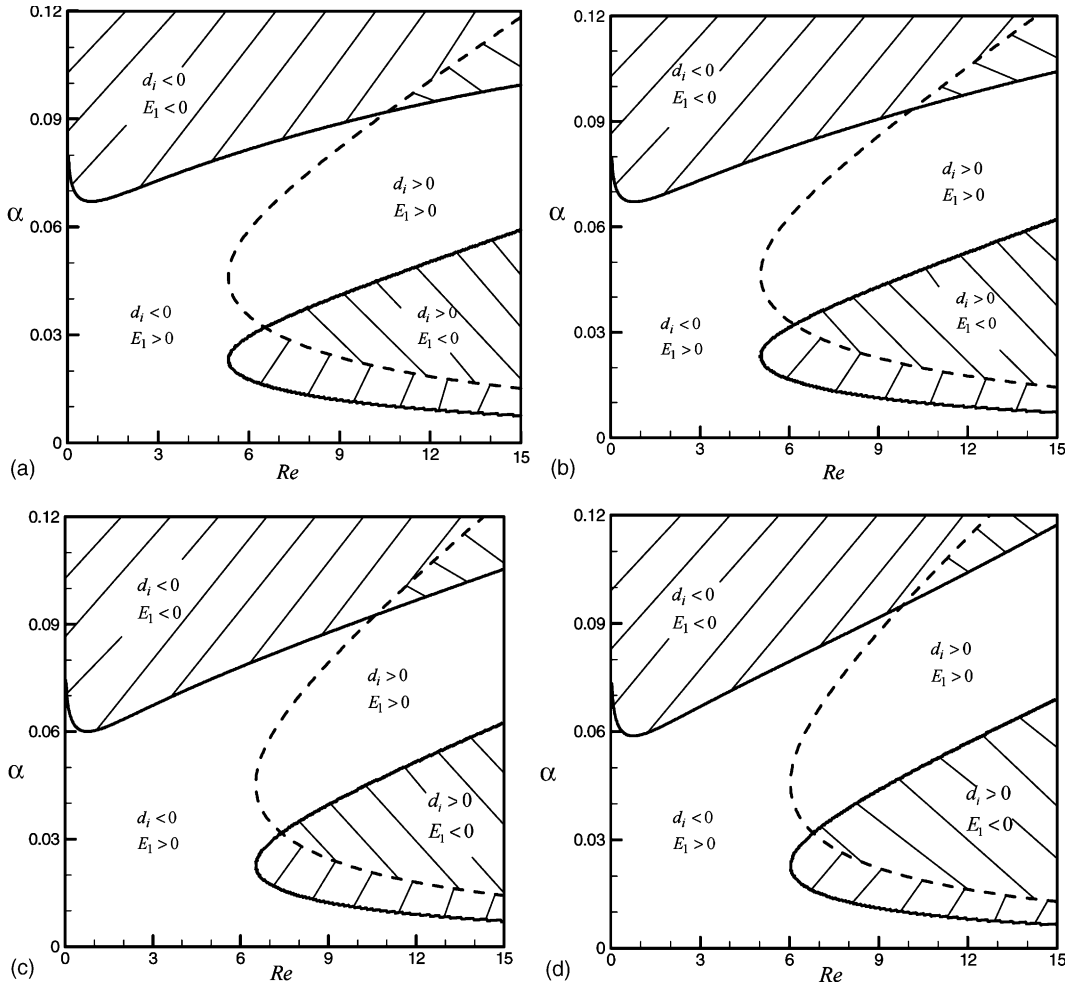

Fig. 6. Neutral stability curve of condensate film flows for (a) $R = 20$, $Ro = 0$; (b) $R = 20$, $Ro = 0.1$; (c) $R = 50$, $Ro = 0.1$; (d) $R = 100$, $Ro = 0.1$.

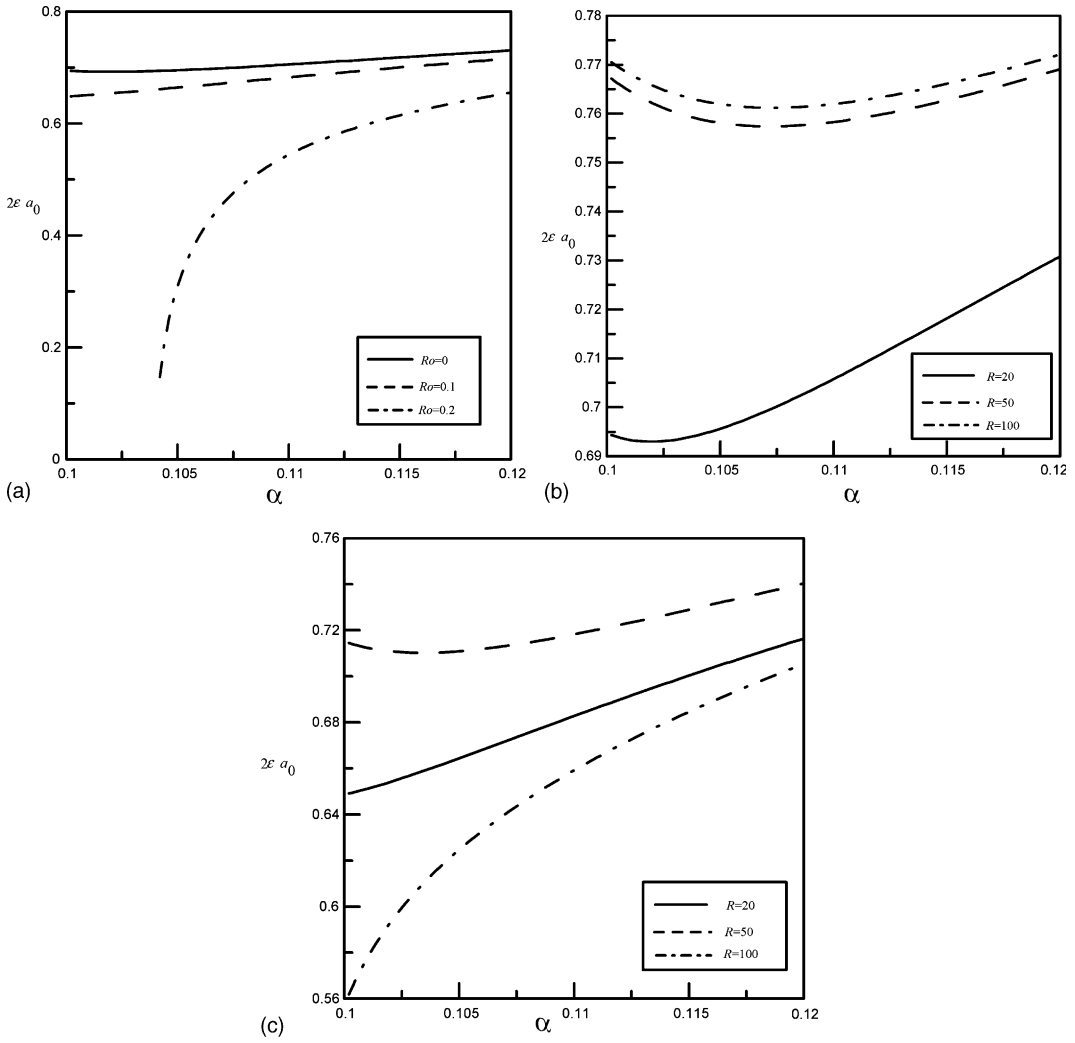

Fig. 7. Threshold amplitude in sub-critical unstable region (a) for three different Ro values at $Re = 10$, $R = 20$; (b) for three different R values at $Re = 10$, $Ro = 0$; (c) $Re = 10$, $Ro = 0.1$.

and the area of sub-critical stability region ($d_i < 0$, $E_1 > 0$) decrease as the values of Ro increase. Fig. 6(b)–(d) show that the neutral stability curves of $d_i = 0$ and $E_1 = 0$ are shifted as the values of R increase when $Ro = 0.1$.

Fig. 7(a) shows the threshold amplitude in sub-critical unstable region for various wave numbers with different Ro values at $Re = 10$ and $R = 20$. The results indicate that the threshold amplitude εa_0 becomes smaller as the value of rotating parameter Ro increases. The film flow which holds the higher threshold amplitude value will become more stable than those hold smaller one. If the initial finite-amplitude disturbance is less than the threshold amplitude, the system will become conditionally stable. Fig. 7(b) shows the threshold amplitude in sub-critical unstable region for various wave numbers with different values of radius R at $Re = 10$ and $Ro = 0$. The results indicate that the threshold amplitude εa_0 becomes smaller as the value of radius R decreasing. In Fig. 7(c), the result shows that the threshold amplitude εa_0 becomes smaller as the value of radius R changing from 50, 20 to 100. This phenomenon is the same as we discuss the results of Fig. 3(a) and (b).

In the linearly unstable region, the linear amplification rate is positive, while the nonlinear amplification rate is negative. Therefore, a linear infinitesimal disturbance in the unstable region, instead of becoming infinite, will reach finite equilibrium amplitude as given in Eq. (40). Fig. 8(a) shows the threshold amplitude in the supercritical stable region for various wave numbers under different values of rotating parameter Ro at

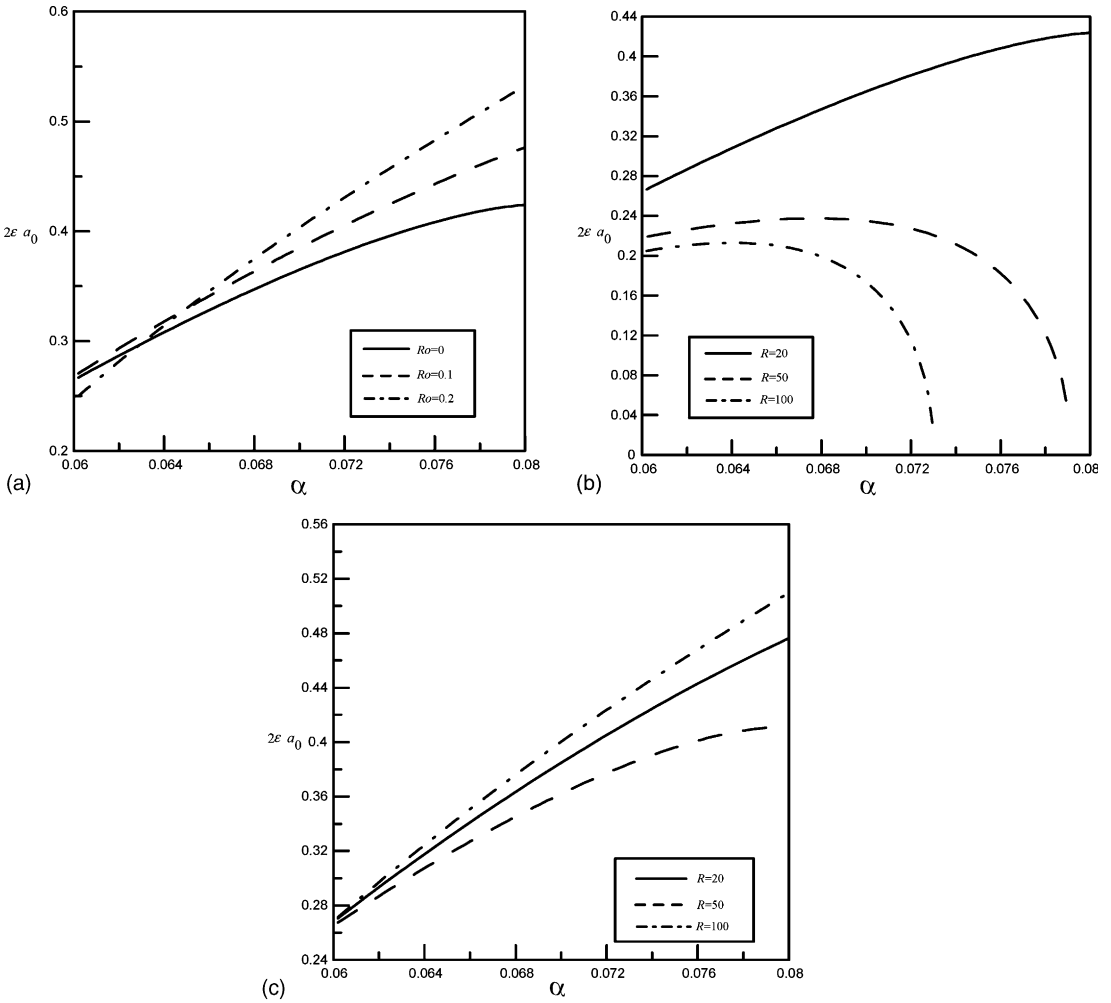

Fig. 8. Threshold amplitude in supercritical stable region (a) for three different Ro values at $Re = 10$, $R = 20$; (b) for three different R values at $Re = 10$, $Ro = 0$; (c) $Re = 10$, $Ro = 0.1$.

$Re = 10$ and $R = 20$. It is found that the decrease of Ro will lower the threshold amplitude, and the flow will become comparatively stable. Fig. 8(b) and (c) show the same conclusion as we reach in the discussion of Fig. 7(b) and (c).

The wave speed of Eq. (28) predicted by using the linear theory is a constant value for all wave number and rotating parameter Ro. However, the wave speed of Eq. (46) predicted by using nonlinear theory is no longer a constant. It is actually a function of wave number, Reynolds number, Rotation number and the radius of cylinder. Fig. 9(a) shows the nonlinear wave speed in the supercritical region for various perturbed wave numbers and different Rotation number $Ro = 0$, 0.1, 0.2 at $Re = 10$ and $R = 20$. It is found that the nonlinear wave speed increases as the value of Ro increases. Fig. 9(b) shows the nonlinear wave speed in the supercritical stable region for various perturbed wave numbers and different cylinder radius $R = 20$, 50 and 100 at $Re = 10$ and $Ro = 0$. Comparing with Fig. 9(b) and (c), the same conclusion about the mutual influence of the cylinder radius and the centrifugal force are also reached. When the cylinder is stationary, the radius dominates the stable characteristics. As the cylinder starts to rotate, the destabilizing influence of centrifugal force should be considered seriously.

5. Conclusions

The stability of a condensate thin film flowing down on the outer surface of a rotating vertical cylinder is

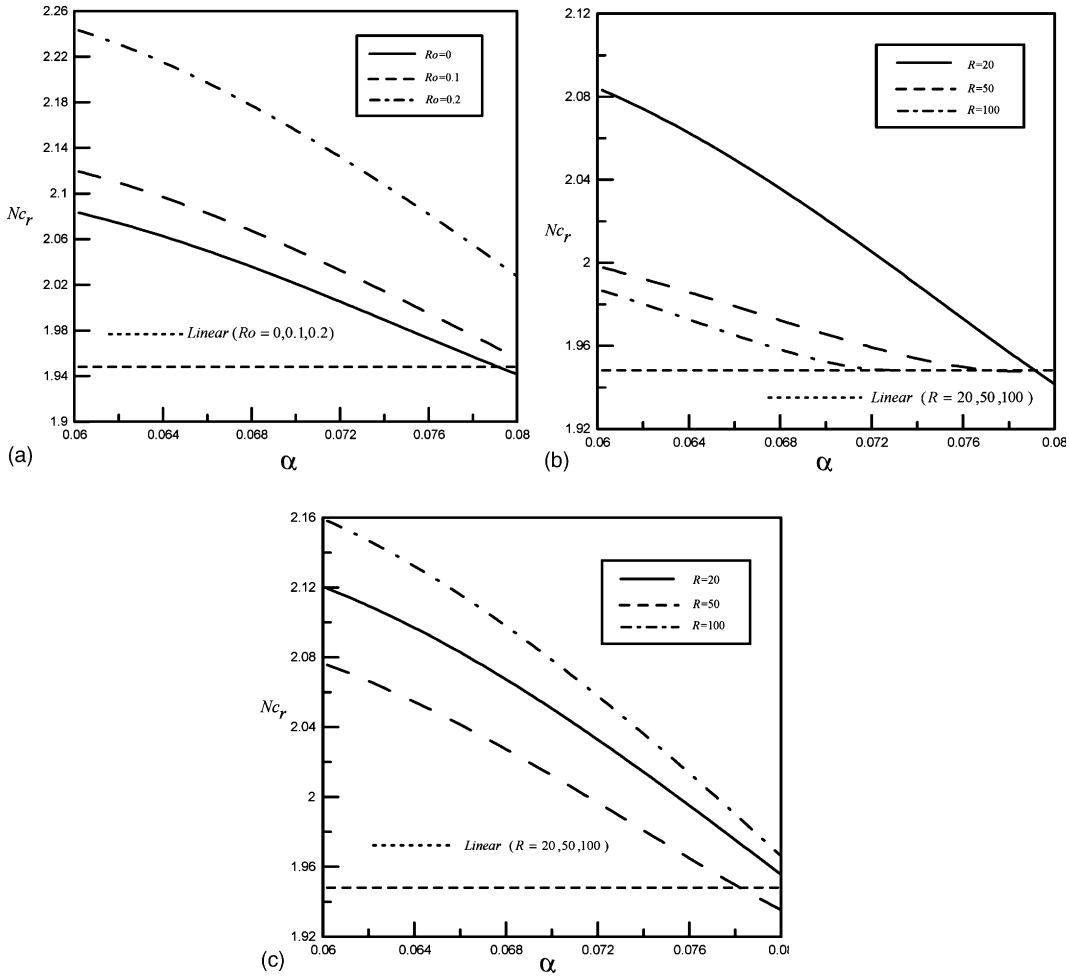

Fig. 9. Nonlinear wave speed in supercritical stable region (a) for three different Ro values at $Re = 10$, $R = 20$; (b) for three different R values at $Re = 10$, $Ro = 0$; (c) $Re = 10$, $Ro = 0.1$.

thoroughly investigated by using the method of long-wave perturbation. Based on the results of numerical modeling, three conclusions can be drawn as follows:

1. The neutral stability curve obtained from linear stability analysis separates the α–Re plane into two different characteristic regions. The modeling results indicate the degree of stability is enhanced if the flow is perturbed by waves with a lower Reynolds number, a lower rotation speed and a greater radius of the cylinder.
2. In the nonlinear stability analysis, it is noted that the area of shaded sub-critical instability region and un-shaded sub-critical stability region decreases as the value of Ro increases and the value of R decreases. On the other hand, the area of shaded supercritical instability region and un-shaded supercritical stability region increases with an increasing Ro value and a decreasing R. It is shown that the threshold amplitude εa_0 in the sub-critical instability region decreases as the value of Rotation number increases for a constant cylinder radius. Both the threshold amplitude and nonlinear wave speed in the supercritical stability region decrease with a decreasing Ro value at the constant radius.
3. The stability behaviors of a thin film flow are significantly affected by the values of Rotation number and radius. The flow field becomes relatively unstable for a large Rotation number and a small radius. When a condensate thin film flows down on the outer surface of a stationary vertical cylinder, the radius of cylinder dominates the stability of flow field only. As the cylinder starts to rotate, the induced centrifugal force should be considered. That is because the radius of cylinder and the rotation speed are mutually influenced. The increasing radius serves as stabilizing factor, but the increasing rotation speed serves as destabilizing factor.

Appendix A

A.1. Zeroth order solution

$$\varphi_0 = \Gamma\left[\frac{1}{4}(r^4+R^4) - \frac{1}{2}R^2r^2 + \frac{1}{2}q^2(r^2-R^2) - q^2r^2\ln\frac{r}{R}\right],$$

$$p_0 = 2S\cdot Re^{-5/3}(2\Gamma)^{1/3}\left(-\alpha^2 h_{zz} + \frac{1}{q}\right)Ro^2R^2\ln\frac{r}{q} - Nd\cdot(Re\cdot\ln Q\cdot q)^{-2},$$

$$\theta_0 = \left(\ln\frac{r}{R}\right)\cdot(\ln Q)^{-1}.$$

A.2. First order solution

$$\varphi_1 = k_1r^6 + k_2r^4 + k_3r^2 + k_4, \quad \theta_1 = b_1r^4 + b_2r^2 + b_3,$$

where

$$k_1 = \tfrac{1}{48}Re\Gamma^2 q h_z,$$

$$k_2 = \frac{1}{8}SRe^{-2/3}(2\Gamma)^{1/3}\left(\alpha^2h_{zzz} + \frac{1}{q^2}h_z\right) + Re\Gamma q h_{0t}\left(\frac{5}{16} - \frac{1}{4}\ln\frac{r}{R}\right) + Re\Gamma^2 q h_z\left\{R^2\left(\frac{3}{16} - \frac{1}{4}\ln\frac{r}{R}\right) + q^2\left[-\frac{3}{2} + \frac{3}{2}\ln\frac{r}{R} - \frac{1}{2}\left(\ln\frac{r}{R}\right)^2\right] - \frac{1}{2}k\right\} + ReRo^2\frac{R^2h_z}{16q},$$

$$k_3 = \frac{1}{4}SRe^{-2/3}(2\Gamma)^{1/3}\left(\alpha^2h_{zzz} + \frac{1}{q^2}h_z\right)\left(q^2 - R^2 - 2q^2\ln\frac{r}{R}\right) + Re\Gamma h_{0t}q\left[q^2\left(\frac{1}{2}\ln Q - \frac{1}{4}\right)\left(2\ln\frac{r}{R} - 1\right) - \frac{1}{2}R^2 + k\left(1 - 2\ln\frac{r}{R}\right)\right] + Re\Gamma^2 q h_z\left\{-\frac{5}{16}R^4 + R^2q^2\left[\frac{5}{2} - \frac{1}{2}\ln\frac{r}{R} + \frac{1}{2}\left(\ln\frac{r}{R}\right)^2\right] + q^4\left[-\frac{7}{8} + \frac{3}{2}\ln Q + \frac{7}{4}\ln\frac{r}{R} - (\ln Q)^2 - 3\ln Q\cdot\ln\frac{r}{R} + 2(\ln Q)^2\ln\frac{r}{R}\right] + k\left[R^2\left(4 - 6\ln\frac{r}{R}\right) + q^2\left(2\ln r - 10\ln R + 8\ln q + 8(\ln r)^2 - 8(\ln R)^2 + 4\left(\ln\frac{r}{R}\right)^2 - 8\ln r\cdot\ln\frac{r}{R} - 8\ln Q\cdot\ln\frac{r}{R} - 8\ln q\cdot\ln\frac{r}{R}\right)\right]\right\} + ReRo^2\frac{R^2}{8q}\left(q^2 - R^2 - 2q^2\ln\frac{r}{R}\right)h_z,$$

$$k_4 = \frac{1}{8}SRe^{-2/3}(2\Gamma)^{1/3}\left(\alpha^2h_{zzz} + \frac{1}{q^2}h_z\right)(R^4 - 2R^2q^2) + Re\Gamma h_{0t}q\left[\frac{3}{16}R^4 + q^2R^2\left(\frac{1}{2}\ln Q - \frac{1}{4}\right) - kR^2\right] + Re\Gamma^2 q h_z\left\{\frac{5}{48}R^6 - R^4q^2 + \frac{1}{8}R^2q^4[7 - 12\ln Q + 8(\ln Q)^2] + k\left[-\frac{7}{2}R^4 + R^2q^2(-2\ln r + 10\ln R - 8\ln q)\right]\right\} + ReRo^2\frac{R^4}{16q}(R^2 - 2q^2)h_z,$$

$$b_1 = \frac{1}{16}Pe\Gamma h_z q^{-1}(\ln Q)^{-2}\left(\ln\frac{r}{2} - \frac{1}{2}\right),$$

$$b_2 = \frac{1}{4}Peh_z q^{-1}(\ln Q)^{-2}\left(1 - \ln\frac{r}{R}\right) + Pe\Gamma h_z q^{-1}(\ln Q)^{-2}\left\{\frac{1}{4}R^2\left(1 - \ln\frac{r}{R}\right) - q^2\left[\frac{1}{2}\left(\ln\frac{r}{R}\right)^2 - \ln\frac{r}{R} + \frac{3}{4}\right]\right\} + Pe\Gamma h_z q(\ln Q)^{-1}\left(\frac{3}{4} - \frac{1}{2}\ln\frac{r}{R}\right),$$

$$b_3 = \frac{1}{4}Peh_{ot}q^{-1}(\ln Q)^{-3}\left[(R^2 + q^2\ln Q - q^2)\ln\frac{r}{R} - R^2\ln Q\right] + \frac{1}{2}PeqR^2\Gamma\ln\frac{r}{R}h_z + \Gamma Pe(\ln Q)^{-1}h_z \times\left\{\left[q^3\ln\frac{r}{R} - \frac{3}{4}qR^2 - \frac{1}{2}qR^2\left(\ln\frac{r}{R}\right)^2\right] + \Gamma(\ln Q)^{-2}Peh_z \times\left[\left(qR^2 - \frac{29}{16}q^3\right)\ln\frac{r}{R} + \left(\frac{3}{4}qR^2 - \frac{7R^4}{32q}\right)\right] + Peh_z\Gamma\ln\frac{r}{R}(\ln Q)^{-3}\left(\frac{25}{32}q^3 - qR^2 + \frac{7R^4}{32q}\right)\right\},$$

where

$$q = R + h,$$

$$Q = \frac{R+h}{R} = \frac{q}{R},$$

$$h_{0t} = 2\Gamma(q^2 - R^2 - 2q^2\ln Q)h_z + \frac{\xi}{\alpha Pe}(1 + \alpha^2h_z^2)q^{-1}(\ln Q)^{-1}.$$

Appendix B. Generalized nonlinear kinematic equation

$$h_t + X(h) + A(h)h_z + B(h)h_{zz} + C(h)h_{zzzz} + D(h)h_z^2 + E(h)h_zh_{zzz} = 0,$$

where

$$X(h) = \frac{\varsigma}{\alpha Pe}[K_1(h) + \varsigma K_2(h)],$$

$$K_1(h) = -q^{-1}(\ln Q)^{-1},$$

$$K_2(h) = -\Big[\tfrac{1}{4}q^{-3}(\ln Q)^{-4}(R^2 - q^2 + q^2\ln Q) - q^{-1}(\ln Q)^{-3}\big(\tfrac{1}{2}\ln Q - \tfrac{1}{4}\big)\Big],$$

$$A(h) = K_3(h) + \varsigma K_4(h) + \frac{\zeta}{Pr}K_5(h),$$

$$K_3(h) = 2\Gamma(R^2 - q^2 + 2q^2\ln Q),$$

$$K_4(h) = \Gamma\Big\{\frac{1}{2}R^2 + \Big(-\frac{1}{4}q^2 - \frac{1}{2}R^2\Big)(\ln Q)^{-1} + \Big(\frac{3}{8}q^2 + \frac{3}{4}R^2\Big)(\ln Q)^{-2} + \frac{9}{32}\Big(-q^2 + \frac{R^4}{q^2}\Big)(\ln Q)^{-3}\Big\},$$

$$K_5(h) = \Gamma\Big\{\big(4q^2 - R^2\big) + \Big(-\frac{9}{4}q^2 + \frac{3}{2}R^2\Big)(\ln Q)^{-1} + \Big(\frac{9}{16}q^2 - \frac{3}{4}R^2 + \frac{3R^4}{16q^2}\Big)(\ln Q)^{-2} - 4q^2\ln Q\Big\},$$

$$B(h) = \alpha SRe^{-2/3}(2\Gamma)^{1/3}K_6(h) + \alpha ReK_7(h) + ReRo^2\alpha K_8(h) + \frac{\alpha Nd}{Re}K_9(h),$$

$$K_6(h) = \frac{1}{8}\Big(4q\ln Q - 3q^3 + 4\frac{R^2}{q} - \frac{R^4}{q^3}\Big),$$

$$K_7(h) = \Gamma^2\Big\{\tfrac{13}{48}R^6 + \tfrac{1}{16}R^4q^2(-9 + 28\ln Q) + \tfrac{1}{48}q^6[59 - 120(\ln Q)^2 + 96(\ln Q)^3] + \tfrac{1}{16}R^2q^4[-15 - 8(\ln q)^2 - 68\ln Q + 16\ln q\cdot\ln Q + 32(\ln Q)^2 + 8(\ln R)^2],$$

$$K_8(h) = \frac{1}{16q^2}R^2(-3q^4 + 4q^2R^2 - R^4 + 4q^4\ln Q),$$

$$K_9(h) = \Big\{\Big(\frac{3}{8} - \frac{R^2}{2q^2} + \frac{R^4}{8q^4}\Big)(\ln Q)^{-3} + \Big(-\frac{1}{8} - \frac{R^2}{4q^2} + \frac{R^4}{8q^4}\Big)(\ln Q)^{-2} - \frac{1}{2}(\ln Q)^{-1}\Big\},$$

$$C(h) = \frac{1}{8}\alpha^3 SRe^{-2/3}(2\Gamma)^{1/3}\Big(4R^2q + 4q^3\ln Q - 3q^3 - \frac{R^4}{q}\Big),$$

$$D(h) = \alpha SRe^{-2/3}(2\Gamma)^{1/3}K_{10}(h) + \alpha ReK_{11}(h) + ReRo^2\alpha K_{12}(h) + \frac{\alpha Nd}{Re}K_{13}(h) + \frac{\alpha\varsigma}{Pe}[K_{14}(h) + \varsigma K_{15}(h)],$$

$$K_{10}(h) = \frac{1}{4}\Big(4\ln Q + \frac{R^4}{q^4} - 1\Big),$$

$$K_{11}(h) = \Gamma^2\Big\{\frac{13R^6}{48q} + q^5\Big[\frac{413}{48} - 5\ln Q - \frac{23}{2}(\ln Q)^2 + 14(\ln Q)^3\Big] + R^4q\Big(\frac{1}{16} + \frac{21}{4}\ln Q\Big) + R^2q^3\Big[-\frac{143}{16} - \frac{65}{4}\ln Q + \frac{25}{2}(\ln Q)^2\Big]\Big\},$$

$$K_{12}(h) = \frac{1}{16q^3}R^2(-5q^4 + 4q^2R^2 + R^4 + 12q^4\ln Q),$$

$$K_{13}(h) = q^{-1}\Big\{-\frac{1}{2}(\ln Q)^{-1} + \Big(\frac{3}{8} + \frac{R^2}{2q^2} - \frac{3R^4}{8q^4}\Big)(\ln Q)^{-2} + \Big(\frac{5}{8} + \frac{3R^2}{2q^2} - \frac{5R^4}{8q^4}\Big)(\ln Q)^{-3} + \Big(-\frac{9}{8} + \frac{3R^2}{2q^2} - \frac{3R^4}{8q^4}\Big)(\ln Q)^{-4}\Big\},$$

$$K_{14}(h) = -(q\ln Q)^{-1},$$

$$K_{15}(h) = q^{-1}\Big[(\ln Q)^{-2} - (\ln Q)^{-3} + \frac{1}{2}\Big(1 - \frac{R^2}{q^2}\Big)(\ln Q)^{-4}\Big],$$

$$E(h) = \alpha^3 SRe^{-2/3}(2\Gamma)^{1/3}(R^2 - q^2 + 2q^2\ln Q).$$

References

[1] W. Nusselt, Die oberflachenkondensation des wasserdampfes, Z. VDI 50 (1916) 541–546.

[2] S.G. Bankoff, Stability of liquid flow down a heated inclined plane, Int. J. Heat Mass Transfer 14 (1971) 377–385.

[3] E. Marschall, C.Y. Lee, Stability of condensate flow down a vertical wall, Int. J. Heat Mass Transfer 16 (1973) 41–48.

[4] M. Ünsal, W.C. Thomas, Linearized stability analysis of film condensation, ASME J. Heat Transfer 100 (1978) 629–634.

[5] D.J. Benney, Long waves on liquid film, J. Math. Phys. 45 (1966) 150–155.

[6] S.P. Lin, Finite amplitude side-band stability of a viscous film, J. Fluid Mech. 63 (1974) 417–429.

[7] C. Nakaya, Equilibrium state of periodic waves on the fluid film down a vertical wall, J. Phys. Soc. Jpn. 36 (1974) 921–926.

[8] M.V.G. Krishna, S.P. Lin, Nonlinear stability of a viscous film with respect to three-dimensional side-band disturbance, Phys. Fluids 20 (1977) 1039–1044.

[9] C.C. Hwang, C.I. Weng, Finite-amplitude stability analysis of liquid films down a vertical wall with and without interfacial phase change, Int. J. Multiphase Flow 13 (1987) 803–814.

[10] W.B. Krantz, R.L. Zollars, The linear hydrodynamic stability of film flow down a vertical cylinder, AIChE J. 22 (1976) 930–934.

[11] P. Rosenau, A. Oron, Evolution and breaking of liquid film flowing on a vertical cylinder, Phys. Fluids A 1 (1989) 1763–1766.
[12] C.I. Hung, C.K. Chen, J.S. Tsai, Weakly nonlinear stability analysis of condensate film flow down a vertical cylinder, Int. J. Heat Mass Transfer 39 (1996) 2821–2829.
[13] T. Takamasa, K. Kobayashi, Measuring interfacial waves on film flowing down tube inner wall using laser focus displacement meter, Int. J. Multiphase Flow 26 (2000) 1493–1507.
[14] D.A. Edwards, H. Brenner, D.T. Wasan, Interfacial Transport Processes and Rheology, Butterworth-Heinemann, a Division of Reed Publishing Inc, USA, 1991.
[15] C.I. Hung, J.S. Tsai, C.K. Chen, Nonlinear Stability of the thin micropolar liquid film flowing down on a vertical plate, ASME J. Fluids Eng. 118 (1996) 498–505.
[16] T.B. Benjamin, Wave formation in laminar flow down an inclined plane, J. Fluid Mech. 2 (1957) 554–574.
[17] C.S. Yih, Stability of liquid flow down an inclined plane, Phys. Fluids 6 (1963) 321–334.
[18] J.S. Tsai, C.I. Hung, C.K. Chen, Nonlinear hydromagnetic stability analysis of condensation film flow down a vertical plate, Acta Mech. 118 (1996) 197–212.
[19] V.L. Ginzburg, L.D. Landau, Theory of superconductivity, J. Exptl. Theoret. Phys. (USSR) 20 (1950) 1064–1082.